Green Chemistry

COMMUNICATION

View Article Online
View Journal | View Issue

Cite this: *Green Chem.*, 2024, **26**, 8680

Received 9th April 2024,
Accepted 25th June 2024

DOI: 10.1039/d4gc01747a

rsc.li/greenchem

Continuous-flow directed C–H amidation reactions using immobilized Cp*Rh(III) catalysts†

Yuki Saito, Taro Konno and Shū Kobayashi *

We report a green, continuous-flow C–H amidation methodology using heterogeneous Cp*Rh(III) catalysts. These catalysts enable halide- and salt-free reactions with excellent activity and durability across diverse substrates, demonstrated by a 200-hour, multi-gram scale reaction exceeding 290 TON (turnover number).

Transition metal-catalyzed C–H bond functionalization has emerged as a powerful and green synthetic method due to its ability to perform efficient chemical transformations under halogen-free and salt-free conditions.[1,2] Recent studies have demonstrated the remarkable potential of this methodology for the synthesis of complex molecules like natural products and active pharmaceutical ingredients (APIs).[3–6] Group 9 Cp*M(III) catalysts, in particular, have been extensively studied and utilized for various C–H functionalization reactions, showcasing their high activity and versatility.[7–11] However, a significant challenge associated with these catalysts is their high cost, often requiring substantial catalyst loading.[12] Additionally, potential contamination of products with toxic metals necessitates further purification steps, leading to increased waste and tedious procedures.

Heterogeneous catalysts offer a solution to these challenges. Their ease of separation and reusability *via* simple filtration promotes efficient syntheses and significantly reduces waste. When coupled with flow chemistry, this approach allows for highly efficient and continuous processes. Recent years have seen the development of diverse heterogeneous catalysts for continuous-flow reactions.[13–16] However, a significant challenge remains: achieving heterogeneous transition metal-catalyzed C–H bond functionalizations in continuous flow. While success has been demonstrated for various continuous-flow reactions using homogeneous catalysts,[17,18] only a few types of heterogeneous catalysts for flow C–H functionalizations have been reported.[19–25] Furthermore, immobilization of Cp*M(III) catalysts, to the best of our knowledge, remains elusive due to the difficulties associated with the process. Notably, the high cost and waste generation associated with traditional methods for modifying the Cp* structure necessitate an immobilization approach that avoids ligand modification altogether.[26]

Building upon our prior development of heterogeneous chiral Rh(I) catalysts for continuous-flow hydrogenation, hydroacylation, enyne cyclization, and chiral Sc(III) catalysts for Friedel–Crafts reactions,[25,27–29] we investigated a novel immobilization method for cationic transition metal complexes using non-covalent interactions. This method has been applied to develop continuous-flow reactions with heterogeneous catalysts. We hypothesized that Cp*Rh(III) could be immobilized using this method due to its cationic nature.

Here, we developed heterogeneous Cp*Rh(III) catalysts for continuous-flow C–H amidation of 2-phenylpyridines.[30] These catalysts can be prepared in batch or flow mode by pumping a metal complex solution into a cartridge column. The catalysts exhibit high activity in C–H amidation for various substrates under continuous-flow conditions, maintaining high performance for at least 200 h of flow reaction without metal leaching.

A three-step synthesis of heterogeneous CpRh(III) catalysts supported on silica is described in Scheme 1.[25,27–29] In the first step, SiO_2 was functionalized with amines (SiO_2-NR_2) using various silane coupling reagents containing primary, secondary, and tertiary amines, as well as dihydroimidazole (H_2-Im). Subsequently, the obtained SiO_2-NR_2 was reacted with heteropoly acids (HPAs) – $H_3PW_{12}O_{40}$ (PTA), $H_4SiW_{12}O_{40}$ (STA), $H_3PMo_{12}O_{40}$ (PMA), and $H_4SiMo_{12}O_{40}$ (SMA) – to form surface-bound acid–base salts (HPA/SiO_2-NR_2). Finally, a Cp*Rh$(NTf_2)_2$ complex, synthesized from $[Cp^*RhCl_2]_2$ and $AgNTf_2$ based on reported procedures,[30] was immobilized onto the HPA/SiO_2-NR_2 supports by stirring in ethyl acetate (EtOAc) for 1 h. This yielded the desired heterogeneous Cp*Rh(III) catalysts (Cp*Rh(III)/HPA/SiO_2-NR_2).

The impact of support structure on the catalytic C–H amidation of 2-phenylpyridine (**1a**) with dioxazolone (**2a**) under

Department of Chemistry, Graduate School of Science, The University of Tokyo, 7-3-1, Hongo, Bunkyo-ku, Tokyo, Japan. E-mail: shu_kobayashi@chem.s.u-tokyo.ac.jp

† Electronic supplementary information (ESI) available. See DOI: https://doi.org/10.1039/d4gc01747a

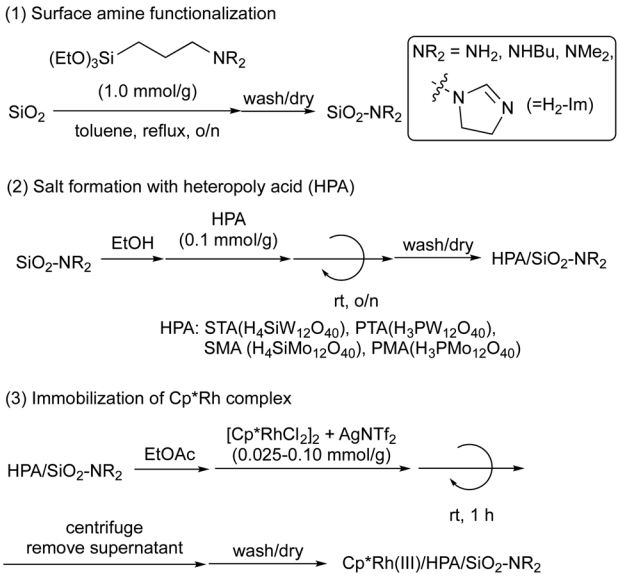

Scheme 1 Catalyst preparation.

batch conditions was evaluated (Table 1). Initially, the effect of heteropoly acids (HPAs) was investigated using a simple primary amine (entries 1–4). STA emerged as the most effective HPA, affording an 85% yield of the desired product **3a**. The highly negatively charged and soft STA^{4-} anion appears to be well-suited for the cationic Cp*Rh(III) catalyst.[31] However, a concerning 7.5% Rh leaching was observed after the reaction. To address Rh leaching, the amine unit structure was subsequently explored. While both primary and secondary amines resulted in lower yields and increased leaching (entries 5 and 6), the use of a dihydroimidazole unit (H_2-Im) led to a gratifying increase in yield and a significant decrease in leaching (entry 7). Based on our prior research, it is hypothesized that the dihydroimidazole unit coordinates with the coordinatively unsaturated Rh(III) center, promoting stabilization and preventing leaching.[29] Finally, the effect of catalyst loading was examined. Decreasing the loading concentration further enhanced the yield and completely suppressed Rh leaching (entries 8 and 9).

We characterized the prepared catalysts using both scanning transmission electron microscope (STEM) analysis and N_2 adsorption/desorption isotherms. STEM revealed good dispersion of Rh, W, and N on the SiO_2 surface, with no observed metal aggregation (Fig. S3†). N_2 adsorption/desorption isotherms confirmed a stepwise decrease in surface area upon SiO_2 functionalization, suggesting that the active Cp*Rh(III) species likely reside on the surface while maintaining the bulk structure of the material (Fig. S1, S2 and Tables S1, S2†).

Leveraging the optimized support structure, we further optimized the reaction under continuous-flow conditions. To achieve this, we developed a continuous-flow immobilization method for heterogeneous catalyst preparation. A $Cp^*Rh(NTf)_2$ solution was pumped through a column reactor packed with STA/SiO_2-H_2-Im, immobilizing the catalyst on the fly. After washing with the reaction solvent, continuous-flow C–H amidation was performed. Initial temperature optimization under continuous-flow revealed a yield improvement to 70% at 80 °C using isoamyl acetate as the solvent (Fig. S4†). Next, we investigated the effect of the Cp* ligand structure (Fig. 1). While Cp and $CpMe_4$ showed similar activity, replacing a methyl group with ^{t}Bu and CF_3 significantly decreased it. The Ind* ligand also exhibited lower activity and durability. These results suggest that catalyst immobilization *via* Cp ligand modification might compromise activity.

Optimizing catalyst and reagent amounts (Fig. 2) significantly increased the yield of **3a** to over 90%. Notably, increas-

Table 1 Catalyst evaluation under batch conditions

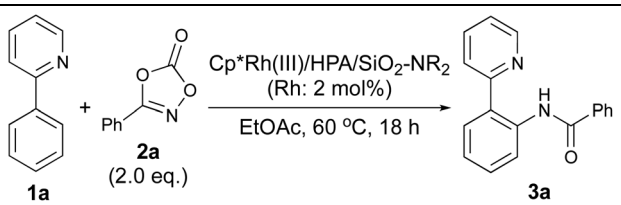

Entry	Amine structure	HPA	Loading (mmol g^{-1})	Yield[a] (%)	Rh leaching[b] (%)
1	NH_2	STA	0.05	85	7.5
2	NH_2	SMA	0.05	32	ND
3	NH_2	PMA	0.05	26	ND
4	NH_2	PTA	0.05	48	ND
5	NH^nBu	STA	0.05	67	1.6
6	NEt_2	STA	0.05	19	1.8
7	H_2-Im	STA	0.05	91	0.5
8	H_2-Im	STA	0.10	90	2.3
9	H_2-Im	STA	0.025	96	UDL

[a] Determined by ^{1}H NMR analysis by using Durene as an internal standard. [b] Determined by ICP analysis.

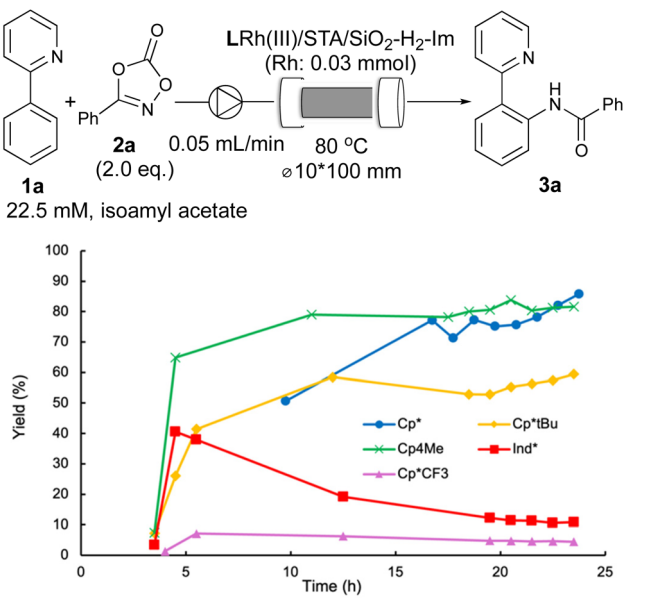

Fig. 1 Effect of Cp ligands.

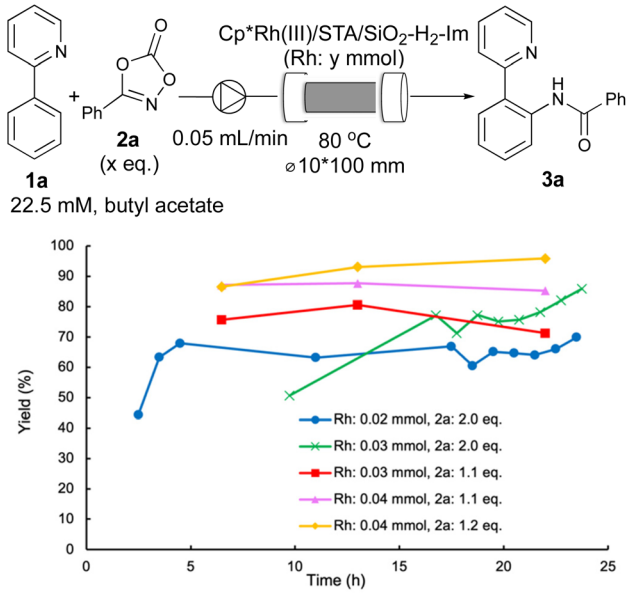

Fig. 2 Effect of amounts of catalyst and **2a**.

ing the catalyst amount while reducing the amount of **2a** from 2.0 to 1.2 equivalents maintained this high yield. Using 0.04 mmol of Rh catalyst and 1.2 equivalents of **2a** achieved this result in a continuous-flow reaction over 24 hours. Importantly, no catalyst deactivation or Rh leaching was observed during the reaction.

With optimized flow conditions established, we investigated the substrate scope using a 42-hour continuous-flow reaction (Scheme 2). The effect of *para*-substituents on the aromatic ring was examined first. Electron-donating groups had minimal impact on reactivity (**3b, c**), while electron-withdrawing groups led to slightly lower yields for target products **3d** and **3e**. This suggests the importance of electron density in the directing pyridine for optimal reactivity. Next, the impact of *meta*-substituents was assessed. Interestingly, both electron-donating and electron-withdrawing groups negatively affected yields (**3f–i**). This observation implies that C–H bond acidity is another crucial factor in substrate reactivity. The scope of amidating reagents (**3**) was also explored. Both electron-donating and electron-withdrawing groups furnished the corresponding products (**3j–l**) in good to excellent yields. However, even a reactive amidating reagent failed to improve the yield for the electron-donating *meta*-substituted substrate (**3m**). This reinforces the notion that pyridine coordination and the subsequent CMD process are central to this reaction.[32] C–H amidation of thiophene was explored, yielding product **3n** in moderate to good yields. Finally, the applicability of other directing groups was tested. Quinoline and isoquinoline were successfully employed, affording products **3o** and **3p**, respectively. Interestingly, using an imidate as a directing group resulted in quinazoline product **3q**, albeit in low to moderate yield. Finally, C–H amidations of indoles were also performed. Regardless of the directing group, the C2-amidtion products **3r** and **3s** were obtained in moderate yields.

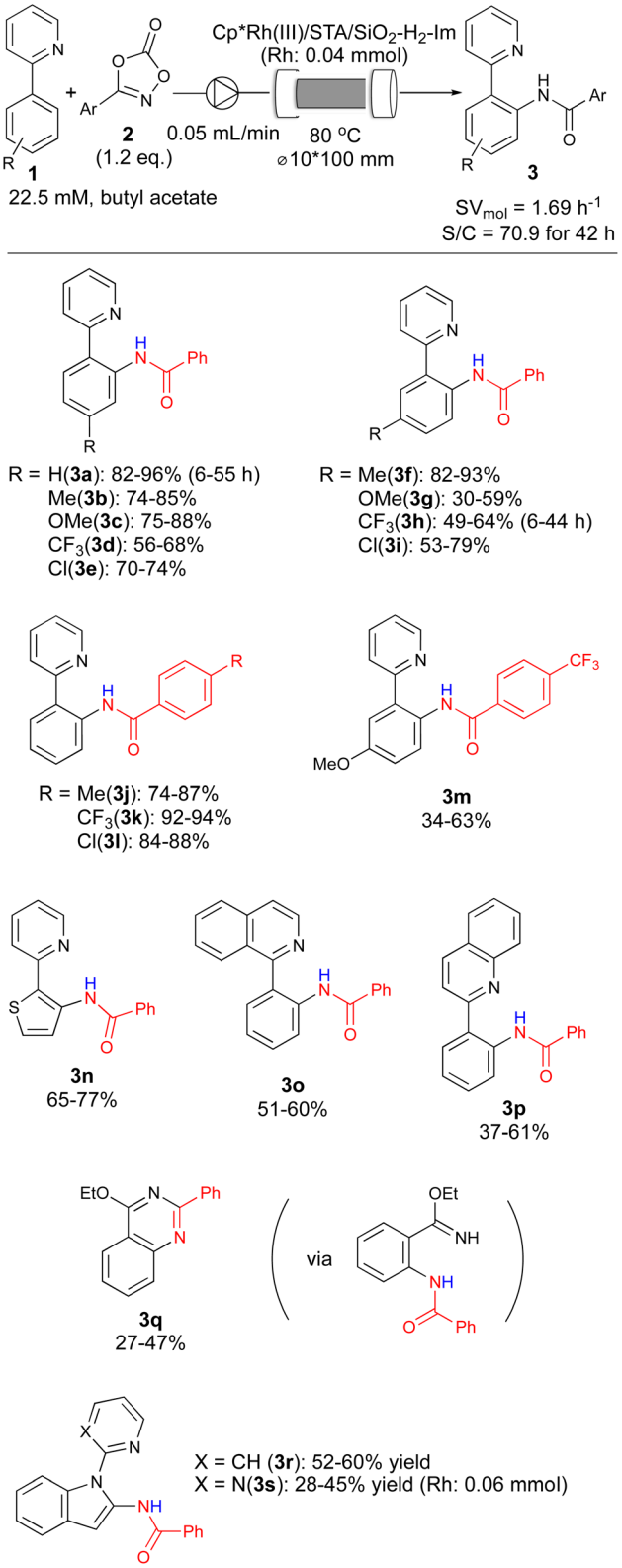

Scheme 2 Substrate scope.

Finally, an extended time continuous-flow experiment was performed to assess the catalyst's durability (Fig. 3). This experiment demonstrated that the target product **3a** could be synthesized in

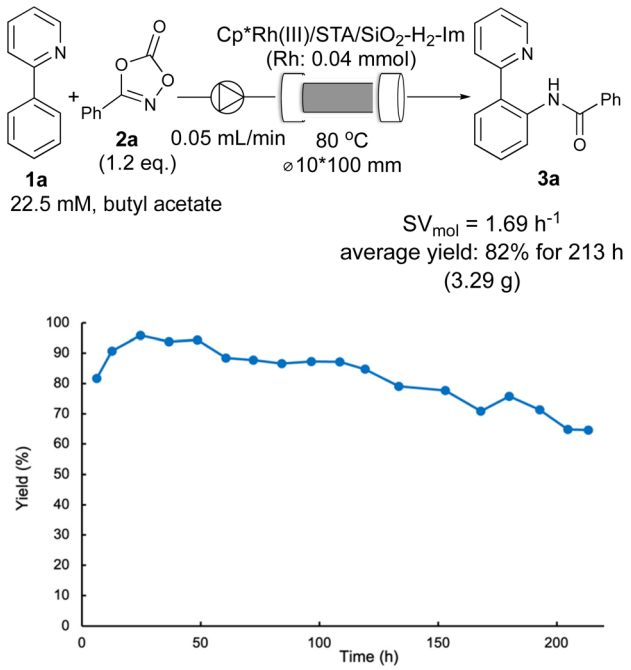

Fig. 3 Extended time flow reaction.

>70% yield for over 200 h continuously. While gradual decrease in catalyst activity was observed over time, this experiment also revealed a total turnover number (TON) exceeding 290. We also attempted to clarify the cause of catalyst deactivation. First and the most importantly, no leaching of the catalyst was observed. STEM and EDS analyses revealed that there was no clear aggregation of Rh species (Fig. S5†). Washing the used catalyst revealed that some polar compounds were adsorbed on the catalyst; however, the activity was not recovered even after washing (Fig. S4, Scheme S7†). Considering the high TON of the homogeneous catalyst under batch conditions (Table S3†), the most plausible cause of the catalyst deactivation is the degradation of the catalyst caused by STA anion or surface amine structure.

In conclusion, we successfully developed heterogeneous Cp*Rh(III) catalysts enabling continuous-flow C–H amidation reactions. Investigation of the support structure revealed that both HPA structure and surface amine are crucial for catalyst activity and preventing leaching. Furthermore, detailed continuous-flow studies highlighted the critical role of the Cp structure in catalyst activity. The optimized reaction conditions resulted in high catalyst activity for various substrates. Notably, the reactions proceeded smoothly under halide-free and salt-free conditions. Finally, extended time flow reactions enabled multigram scale synthesis without catalyst leaching. Further investigations to clarify the cause of catalyst deactivation and improve the catalyst durability are under investigation.

Data availability

The data supporting this article have been included as part of the ESI.†

Conflicts of interest

There are no conflicts to declare.

Acknowledgements

This work was supported in part a The Grant-in-Aid for Transformative Research Areas (A) JP21A204/22H05345 Digitalization-driven Transformative Organic Synthesis (Digi-TOS) from the Ministry of Education, Culture, Sports, Science & Technology, Japan. We thank Dr Tei Maki (The University of Tokyo and JEOL) for STEM and EDS analyses.

References

1 D. Maiti, *Handbook of CH-Functionalization*, Wiley-VCH GmbH, 2022.
2 T. Punniyamurthy and A. Kumar, *Transition-Metal-Catalyzed C-H Functionalization of Heterocycles*, Wiley-VCH GmbH, 2023.
3 R. R. Karimov and J. F. Hartwig, *Angew. Chem., Int. Ed.*, 2018, **57**, 4234–4241.
4 D. J. Abrams, P. A. Provencher and E. J. Sorensen, *Chem. Soc. Rev.*, 2018, **47**, 8925–8967.
5 M. Moir, J. J. Danon, T. A. Reekie and M. Kassiou, *Expert Opin. Drug Discovery*, 2019, **14**, 1137–1149.
6 L. Guillemard, N. Kaplaneris, L. Ackermann and M. J. Johansson, *Nat. Rev. Chem.*, 2021, **5**, 522–545.
7 G. Song and X. Li, *Acc. Chem. Res.*, 2015, **48**, 1007–1020.
8 T. Yoshino and S. Matsunaga, *Adv. Synth. Catal.*, 2017, **359**, 1245–1262.
9 T. Piou and T. Rovis, *Acc. Chem. Res.*, 2017, **51**, 170–180.
10 T. Yoshino, S. Satake and S. Matsunaga, *Chem. – Eur. J.*, 2020, **26**, 7346–7357.
11 S. Y. Hong, Y. Hwang, M. Lee and S. Chang, *Acc. Chem. Res.*, 2021, **54**, 2683–2700.
12 U. Dhawa, N. Kaplaneris and L. Ackermann, *Org. Chem. Front.*, 2021, **8**, 4886–4913.
13 R. Munirathinam, J. Huskens and W. Verboom, *Adv. Synth. Catal.*, 2015, **357**, 1093–1123.
14 A. Tanimu, S. Jaenicke and K. Alhooshani, *Chem. Eng. J.*, 2017, **327**, 792–821.
15 K. Masuda, T. Ichitsuka, N. Koumura, K. Sato and S. Kobayashi, *Tetrahedron*, 2018, **74**, 1705–1730.
16 W.-J. Yoo, H. Ishitani, Y. Saito, B. Laroche and S. Kobayashi, *J. Org. Chem.*, 2020, **85**, 5132–5145.
17 S. Santoro, F. Ferlin, L. Ackermann and L. Vaccaro, *Chem. Soc. Rev.*, 2019, **48**, 2767–2782.
18 S. Govaerts, A. Nyuchev and T. Noel, *J. Flow Chem.*, 2020, **10**, 13–71.
19 T. Tagata, M. Nishida and A. Nishida, *Adv. Synth. Catal.*, 2010, **352**, 1662–1666.
20 H. P. L. Gemoets, G. Laudadio, K. Verstraete, V. Hessel and T. Noël, *Angew. Chem., Int. Ed.*, 2017, **56**, 7161–7165.

21 F. Ferlin, S. Santoro, L. Ackermann and L. Vaccaro, *Green Chem.*, 2017, **19**, 2510–2514.
22 C. J. Yoo, D. Rackl, W. Liu, C. B. Hoyt, B. Pimentel, R. P. Lively, H. M. L. Davies and C. W. Jones, *Angew. Chem., Int. Ed.*, 2018, **57**, 10923–10927.
23 F. Ferlin, L. Luciani, S. Santoro, A. Marrocchi, D. Lanari, A. Bechtoldt, L. Ackermann and L. Vaccaro, *Green Chem.*, 2018, **20**, 2888–2893.
24 F. Ferlin, I. Anastasiou, N. Salameh, T. Miyakoshi, O. Baudoin and L. Vaccaro, *ChemSusChem*, 2022, **15**, 1–7.
25 Y. Saito and S. Kobayashi, *Angew. Chem., Int. Ed.*, 2023, **63**, e202313778.
26 J. M. Fraile, J. I. García and J. A. Mayoral, *Chem. Rev.*, 2008, **109**, 360–417.
27 Y. Saito and S. Kobayashi, *J. Am. Chem. Soc.*, 2020, **142**, 16546–16551.
28 Y. Saito and S. Kobayashi, *Angew. Chem., Int. Ed.*, 2021, **60**, 26566–26570.
29 Y. Saito, Y. Sato and S. Kobayashi, *ACS Catal.*, 2024, **14**, 2202–2206.
30 Y. Park, K. T. Park, J. G. Kim and S. Chang, *J. Am. Chem. Soc.*, 2015, **137**, 4534–4542.
31 M. N. Timofeeva, *Appl. Catal., A*, 2003, **256**, 19–35.
32 Y. Park, K. T. Park, J. G. Kim and S. Chang, *J. Am. Chem. Soc.*, 2015, **137**, 4534–4542.